A Brief Analysis of the Motion Compensation for FMCW SAR

Jia Gaowei
School of Electronic Science and Engineering
National University of Defense Technology
Changsha, China
jiagaoweinudt@gmail.com

Chang Wenge, Li Xiangyang and Zhao Zhiyong
School of Electronic Science and Engineering
National University of Defense Technology
Changsha, China
changwenge@nudt.edu.cn, lxyniu@sina.com,
zhaozhiyong.1983@gmail.com

***Abstract*—The combination of frequency modulated continuous wave (FMCW) and SAR (synthetic aperture radar) , is one of the most important and dynamic research around the world. For FMCW SAR, traditional approximation of stop-go is invalid, hence the traditional motion compensation method is no longer suitable for FMCW SAR. The signal model of FMCW SAR in the presence of motion error is derived in the paper, as well as the difference introduced by inter-pulse motion errors. Then a new motion compensation method is proposed. Simulated and experimental FMCW SAR data is generated and the well-focused image shows the proposed method is available.**

Keywords-Frequency Module Continuous Wave; Synthetic Aperture Radar; Motion Compensation; Line of Sight; intra-pulse; inter-pulse.

I. INTRODUCTION

Being a kind of advanced imaging sensor, SAR has been assembled with a variety of platforms, like airplane, airship, helicopter, missile, UAV (unmanned airplane vehicle), even the satellites. Most of these airborne platforms would be disturbed by the air current and are going to move on a non-ideal trajectory, accordingly, declines the quality of SAR imagery, even leads to a failure of imaging.

Airplane is a popular platform for SAR system, in the background of the glorious boom of UAVs, the combination of SAR and UAV, leads to a significant development for both the SAR sensor and UAVs. For one thing, it expands the application of SAR, for another, UAVs could have a stronger power of observation. However, the limited load of UAV could not satisfy the big, heavy and high-power pulsed SARs. Fortunately, the technology of FMCW could make the SAR smaller, low power and low-weight. It is the reason why FMCW SAR has been one of the most important and dynamic research in the field of radar around the world [1-5].

In FMCW SAR Systems，due to the fact that the transmitted wave is continuous and the length is in milliseconds, traditional approximation of stop-go in SAR theory is no longer valid. The motion during inter-pulse could not be ignored and the original method of motion compensation is not available either. But the error motion could still be separated into two terms: range error along the LOS and velocity error along track. Resampling the raw data along the track or transmitting the pseudo-continuous wave whose duty cycle is approximately to 1 then adjusting the PRF online are alternative for the elimination of velocity error. Thus the processing of eliminating velocity error could be seen as the preparation for imaging. However, it becomes complicated when dealing with the range error. A new method which is available for compensating the range error is proposed in this paper. In addition, a laboratorial FMCW SAR system is built-up, based on which the presented approach could be validated.

In Section II, the SAR system geometry and signal in presence of trajectory deviation is addressed. In Section III, difference phenomenon introduced by inter-pulse motion error is presented while the related approach is presented too. The proposed method is verified with the simulated and experimental data in Section IV. Finally, the conclusion is pointed out in Section V.

II. SIGNAL MODEL OF FMCW SAR IN NON-IDEAL CASE

Let us refer to Fig.1, in which the SAR system geometry in the presence of the 3-D motion error is presented. The real trajectory is shown as the dotted line, while the straight line along X denotes the ideal trajectory. O means the origin of the coordinates and β is the off-nadir angle. $P_e(X(t),Y(t),Z(t))$ are the azimuth, range and height position of the antenna phase center (APC), while $\Delta X(t),\Delta Y(t),\Delta Z(t)$ are the instantaneous 3-D error. $R(t,R_B)$ denotes the instantaneous range target-to-antenna distance and t is the time variable within time axis. It could be expressed as $t=\hat{t}+t_m$, in which $\hat{t}$ is the fast time and t_m is the slow time.

Assuming the static target T in the scene, whose position is $[X_n,Y_n,Z_n]$, then the instantaneous range between T and APC is

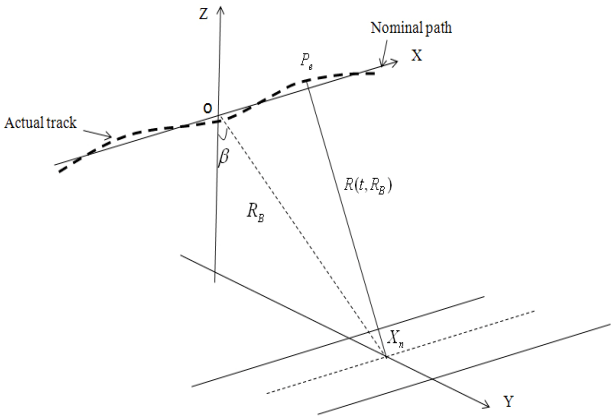

Figure.1. FMCW SAR system geometry in presence of trajectory deviation

$$R(t,R_B)=\sqrt{(X(t)-X_n)^2+(\Delta Y(t)-Y_n)^2+(\Delta Z(t)-Z_n)^2} \quad (1)$$

Correspondingly, $R(t,R_B)$ would be expressed in ideal case as

$$R(t,R_B)=\sqrt{(Vt-X_n)^2+Y_n^2+Z_n^2}=\sqrt{(Vt-X_n)^2+R_B^2} \quad (2)$$

where V means the ideal velocity, and $R_B=\sqrt{Y_n^2+Z_n^2}$ denotes the distance of closest approach. The expression shown in (2) reveals that the varied points at the same range have the same closest distance and they will have a similar signal form. It is known as invariance of azimuth and made the range cell migration compensation more convenient and quick. Unfortunately, the motion error destroys the invariance and convenience.

As $|\Delta Y(t)\sin\beta+\Delta Z(t)\cos\beta|<<\sqrt{(X(t)-X_n)^2+R_B^2}$, (1) could be expressed after the Taylor expansion as

$$\begin{aligned}R(t,R_B)&=\sqrt{(X(t)-X_n)^2+R_B^2-2\Delta Y(t)R_B\sin\beta-2\Delta Z(t)R_B\cos\beta+\Delta Y^2(t)+\Delta Z^2(t)}\\&\approx\sqrt{(X(t)-X_n)^2+R_B^2-2\Delta Y(t)R_B\sin\beta-2\Delta Z(t)R_B\cos\beta}\\&=\sqrt{(X(t)-X_n)^2+R_B^2}\cdot\sqrt{1-\frac{2R_B[\Delta Y(t)\sin\beta+\Delta Z(t)\cos\beta]}{(V_xt-X_n)^2+R_B^2}}\\&\approx\sqrt{(X(t)-X_n)^2+R_B^2}-\frac{R_B}{\sqrt{(V_xt-X_n)^2+R_B^2}}[\Delta Y(t)\sin\beta+\Delta Z(t)\cos\beta]\\&=\sqrt{(X(t)-X_n)^2+R_B^2}-\Delta r(t,R_B)\cos\theta\end{aligned} \quad (3)$$

where

$\cos\theta=\dfrac{R_B}{\sqrt{(V_xt-X_n)^2+R_B^2}}\approx\dfrac{R_B}{\sqrt{(V_xt_m-X_n)^2+R_B^2}}$, θ is the instantaneous squint angle between APC and scatter T. The first approximation in (3) is derived from the situation that $\max\{\Delta Y(t),\Delta Z(t)\}<<R_B$ and the second approximation benefit from the ignorance of the second and senior order term, most importantly, these approximations are available generally.

In (3) it is denoted that the 3-D motion error has been separated into cross-track and along-track motion error. (3) Could be expressed as follows in the case that ignoring the inter-pulse motion, exactly for the pulsed SAR,

$$R(t_m,R_B)=\sqrt{(X(t_m)-X_n)^2+R_B^2}-\Delta r(t_m,R_B)\cdot\cos\theta \quad (4)$$

in which t_m denotes the slow time, being a sample of the whole time t. $X(t_m)$ is the azimuth location of platform for pulsed SAR. $\Delta r(t_m,R_B)=\Delta Y(t_m)\sin\beta+\Delta Z(t_m)\cos\beta$. Intuitively, (4) could be obtained by exchanging t with t_m and the process is shown in Fig.2.

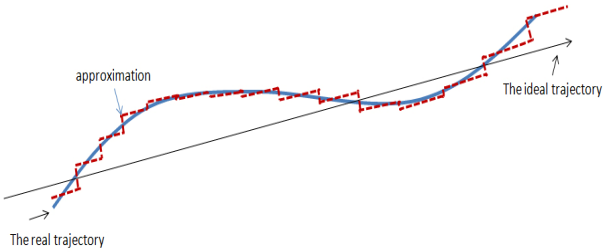

Figure.2. The real and sampled result of trajectory. The black thin straight line means the ideal trajectory and the thick line denotes the real trajectory while the dotted line is the sampled result, using PRI as the interval.

The sampled line is suitable for pulsed SAR but unavailable for FMCW SAR due to the fact that the inter-pulse motion error could not be ignored.

For FMCW SAR, assuming the period of the transmitted LFM is T_r, which is on the order of $10^{-4}s$. It is reasonable to consider the velocity contains same during T_r, shown as $V(t_m+\hat{t})=V(t_m),V_r(t_m+\hat{t})=V_r(t_m)\ \ \hat{t}\in[0,T_r]$, in which V_r means the velocity of platform along LOS. Consequently, (3) is separated as

$$\begin{aligned}R(t,R_B)&=\sqrt{(X(t)-X_n)^2+R_B^2}-\Delta r(t,R_B)\cos\theta\\&\approx\sqrt{(X(t)-X_n)^2+R_B^2}-\Delta r(t_m,R_B)\cos\theta\\&\quad-(V_y(t_m)\sin\beta\cdot\hat{t}+V_z(t_m)\cos\beta\cdot\hat{t})\cos\theta\\&\approx\sqrt{(X(t)-X_n)^2+R_B^2}-\Delta r(t_m,R_B)-\xi_{t_m}\cdot\hat{t}\end{aligned} \quad (5)$$

where $\xi_{t_m}=V_y(t_m)\sin\beta+V_z(t_m)\cos\beta$, the first approximation is available in the case of $\Delta Y(t)\approx\Delta Y(t_m)+V_y(t_m)\hat{t}$, $\Delta Z(t)\approx\Delta Z(t_m)+V_z(t_m)\hat{t}$ while the second one is $\cos\theta\approx1$, especially satisfied for high-band SAR.

The raw echo of FMCW SAR in the ideal case is [2-3]

$$\begin{aligned}s(\hat{t},t_m)&=w_r[\hat{t}-\frac{2R(t)}{c}]w_a[t_m]\exp(-j\frac{4\pi}{\lambda}R(t,R_B))\\&\quad\exp(-j\frac{4\pi k}{c}\hat{t}\cdot R(t,R_B))\exp(j\frac{4\pi kR^2(t,R_B)}{c^2})\end{aligned} \quad (6)$$

(6) is approximated usually as

$$\begin{aligned}s(\hat{t},t_m)&=\{w_r[\hat{t}]w_a[t_m]\exp(-j\frac{4\pi}{\lambda}R(t,R_B))\exp(-j\frac{4\pi k}{c}\hat{t}\cdot R(t,R_B))\\&\quad\}\otimes\exp(-j\pi k\hat{t}^2)\end{aligned} \quad (7)$$

where $w_r[\hat{t}],w_a[t_m]$ are the rectangle envelopes of echo in range and azimuth dimension respectively (ignoring the inference of antenna's weight). Substituting (5) into (6), the signal model of FMCW SAR which is in the presence of motion errors is derived. Since the range error has a negligible effects on the envelop, same to the inter-pulse motion error on RVP term, the finally echo is

$$
\begin{aligned}
s(\hat{t},t_m) = {} & w_r[\hat{t}-\frac{2R(t)}{c}]w_a[t_m]\exp(-j\frac{4\pi}{\lambda}R_1(t,R_B))\exp(j\frac{4\pi}{\lambda}\Delta r(t_m,R_B)) \\
& \exp(j\frac{4\pi}{\lambda}\xi_{t_m}\cdot\hat{t})\exp(-j\frac{4\pi k}{c}\hat{t}\cdot R_1(t,R_B))\exp(j\frac{4\pi k}{c}\hat{t}\cdot\Delta r(t_m,R_B)) \\
& \exp(j\frac{4\pi k}{c}\xi_{t_m}\cdot\hat{t}^2)\exp(j\frac{4\pi k R_1^2(t_m,R_B)}{c^2}) \\
& \exp(j\frac{8\pi k R_1(t_m,R_B)}{c^2}\cdot\Delta r(t_m,R_B))\exp(j\frac{4\pi k\Delta r^2(t_m,R_B)}{c^2})
\end{aligned} \tag{8}
$$

where $R_1(t,R_B)=\sqrt{(X(t)-X_n)^2+R_B^2}$, $R_1(t_m,R_B)=\sqrt{(X(t_m)-X_n)^2+R_B^2}$ and (8) is the basic of motion compensation for FMCW SAR.

III. THE DIFFERENCE INTRODUCED BY INTER-PULSE MOTION

Since the motion error along track could be eliminated respectively, this paper is concentrated on method of how to deal with the cross-track error. It is reasonable to believe that the along track error has been eliminated here. Ignoring tiny terms $\exp(j\frac{4\pi k}{c}\xi_{t_m}\cdot\hat{t}^2)$ and $\exp(j\frac{4\pi k\Delta r^2(t_m,R_B)}{c^2})$, (8) is simplified as

$$
\begin{aligned}
s_1(\hat{t},t_m) = {} & w_r[\hat{t}-\frac{2R(t)}{c}]w_a[t_m]\exp(-j\frac{4\pi}{\lambda}R_0(t,R_B))\exp(j\frac{4\pi}{\lambda}\Delta r(t_m,R_B)) \\
& \exp(j\frac{4\pi}{\lambda}\xi_{t_m}\cdot\hat{t})\exp(-j\frac{4\pi k}{c}\hat{t}\cdot R_0(t,R_B))\exp(j\frac{4\pi k}{c}\hat{t}\cdot\Delta r(t_m,R_B)) \\
& \exp(j\frac{4\pi k R_0^2(t_m,R_B)}{c^2})\exp(j\frac{8\pi k R_0(t_m,R_B)}{c^2}\cdot\Delta r(t_m,R_B))
\end{aligned} \tag{9}
$$

where $R_0(t,R_B)=\sqrt{(Vt-X_n)^2+R_B^2}$, $R_0(t_m,R_B)=\sqrt{(Vt_m-X_n)^2+R_B^2}$.

After a simplification and approximation, (9) changes to

$$
\begin{aligned}
s_1(\hat{t},t_m) \approx {} & \{w_r[\hat{t}]w_a[t_m]\exp(-j\frac{4\pi}{\lambda}R_1(t,R_B))\exp(-j\frac{4\pi k}{c}\hat{t}\cdot R_1(t,R_B)) \\
& \exp(j\frac{4\pi}{\lambda}\Delta r_R(t_m,R_B))\exp(j\frac{4\pi k}{c}\hat{t}\Delta r_R(t_m,R_B)) \\
& \exp(j\frac{4\pi}{\lambda}\xi_{t_m}\cdot\hat{t})\}\otimes\exp(-j\pi k\hat{t}^2)
\end{aligned} \tag{10}
$$

The convolution term outsides the bracket represents the RVP and envelop oblique terms, introduced by the de-chirp processing, which shall be eliminated in the process of imaging. Referring to (10), it is known that the errors due to range error along LOS is

$$
H_{los}=\exp(j\frac{4\pi}{\lambda}\Delta r_R(t_m,R_B))\exp(j\frac{4\pi k}{c}\hat{t}\Delta r_R(t_m,R_B))\exp(j\frac{4\pi}{\lambda}\xi_{t_m}\cdot\hat{t}) \tag{11}
$$

Specifically, the first two terms are introduced by intra-pulse motion and the last one is derived from the inter-pulse motion. The traditional approach could handle the former terms but be unavailable for the latter. The complete expression of $\exp(j\frac{4\pi}{\lambda}\xi_{t_m}\cdot\hat{t})$ is

$$
H_{\xi}=\exp(j\frac{4\pi}{\lambda}\xi_{t_m}\cdot\hat{t})=\exp\{j\frac{4\pi}{\lambda}[V_y(t_m)\sin\beta+V_z(t_m)\cos\beta]\cdot\hat{t}\} \tag{12}
$$

(12) is a function of $\hat{t}$ and be linear with it, whose influence is to introduce new range cell migration, expressed as

$$
\Delta Rcm=\frac{c}{2k}\cdot\frac{2}{\lambda}[V_y(t_m)\sin\beta+V_z(t_m)\cos\beta] \tag{13}
$$

where c represents the speed of light, k denotes the chirp rate. Since $V_y(t_m)$, $V_z(t_m)$ and β vary along azimuth and range respectively, so ΔRcm is changing in two-dimensional, increasing the difficulty to compensate quickly and completely. Fortunately, $V_y(t_m)$ and $V_z(t_m)$ are not very large, then a substituted method is compensating the whole scene with the range cell migration calculated in the center of scene, which is

$$
\Delta Rcm(t_m,R_c)=\frac{c}{2k}\cdot\frac{2}{\lambda}[V_y(t_m)\sin\beta_c+V_z(t_m)\cos\beta_c] \tag{14}
$$

where β_c denotes the off-nadir angle according to the center of scene.

As for the real-time processing of SAR, the approach of motion compensation and imaging are merged to pursuit the maximum efficiency. Due to the fact that range doppler (RD) algorithm is effectively and easy to realize, an available approach of motion compensation which is based on RDA is proposed in this paper, and the flow chart is shown in Fig. 3:

The flow chart of imaging process with motion compensation is similar with pulsed SAR exception for

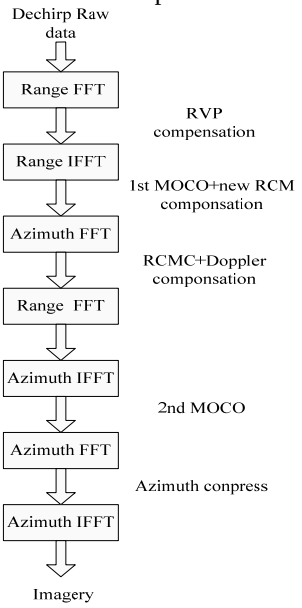

Figure.3. The flow chart of imaging process

TABLE.1: PARTIAL PARAMETERS OF SIMULATION

Range bandwidth	600MHz	altitude	700m
Maximum range	1120m	Minimum range	910m
Pulse duration	800us	velocity	30m/s

the terms of new RCM compensation, and the compensation of Doppler factor. The form of first and second ordered motion compensation could quote from [6][8], the two-step motion compensation method is used widely in data focusing. It's necessary to point out that the Doppler factor is derived from the continuous move inter-pulse and be considered as the main difference between pulsed SAR and FMCW SAR.

IV. THE RESULTS OF SIMULATION AND EXPERIMENT

It is common for airplane to be disturbed by the air current, especially, severe and high-frequency jitter would made the velocity error obvious and increase the difficulty for compensation. Firstly, partial parameters of simulation are settled in Table 1.

Assuming the location error in Y dimension obey a sine wave whose amplitude and period are 3m and 5s, while the location error in Z dimension obey a cosine wave whose amplitude and period are 4m/s and 5s. Then the velocity error could be calculated by the difference of location error. Both of them are shown in Fig. 4.

Based on (13) and the parameters in Table 1, we could calculate the new RCM introduced by inter-pulse motion errors, shown in Fig. 5.

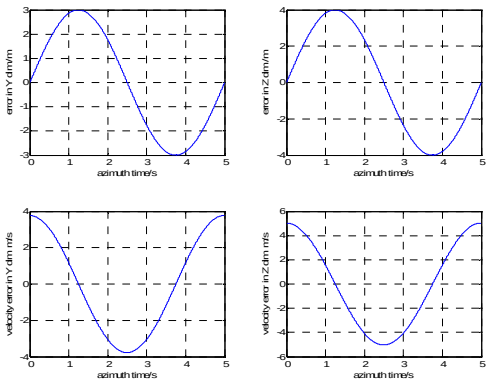

Figure.4 Location and velocity errors in Y and Z dimensions

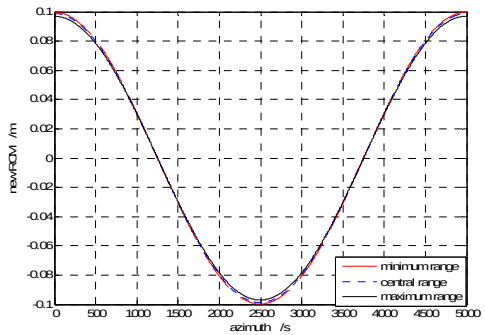

Figure.5. the new RCMs introduced by inter-pulse motion error

There are two conclusions can be derived from Fig. 5; for one thing, the absolute value of new RCM is about 0.2m which will has a obvious influence to imagery when the range resolution is less than 0.2m. For the other, referring to the parameter in Table.1, the difference of new RCM from minimum range or maximum range to central range are tiny, hence compensating the whole scene with (14) is available.

Fig.6 shows the result of an analysis of simulated FMCW SAR data. Fig.6 (a) shows the distribution of scatters. Fig.6 (b) shows the motion correction result using traditional compensation method, whereas Fig.6 (c) shows the motion correction result using the proposed compensation method. An array of point targets is used for the qualitative analysis, especially for the points located in the margin and center of scene. The proposed motion compensation is compared to traditional motion correction method in the presence of severe motion error. The better results performed by proposed method represent the better applicability for FMCW SAR.

From the theoretical analysis and simulated result, it has been seen that the proposed method is valid to compensate the motion errors when the resolution is very high and the motion error is severe. Although when the resolution is low and the trajectory is better, new range migration derived from (13) is less than half of range resolution, the new range migration derived from inter-pulse motion error could be ignored.

The experiment was also carried out with our designed FMCW SAR system, in which the SAR system is fixed on the roof of a sport utility vehicle (SUV), the LFM bandwidth is 600MHz, some corner reflectors were placed

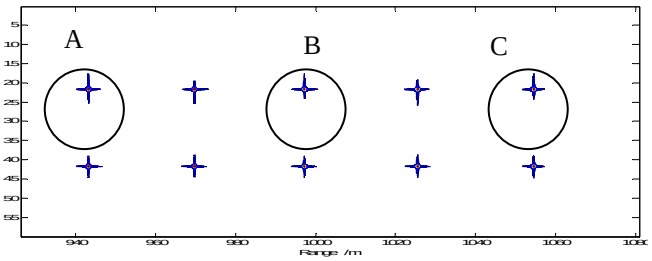

(a) The image of scatters

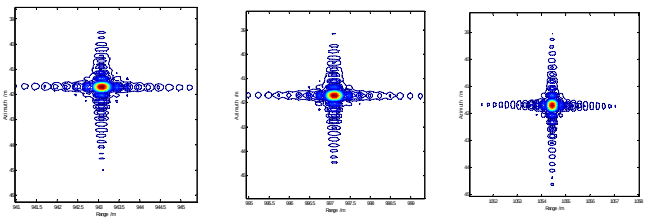

(b) From left to right are A, B, C point.

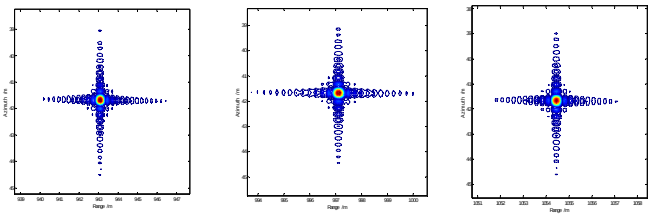

(c) From left to right are A, B, C point.

Figure.6. Simulated FMCW SAR data of an array of point targets and different results are compared with two methods.

 ISBN: 978-1-61208-264-6

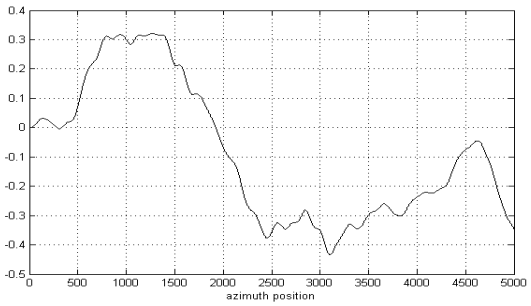

(a) Measured displacement from the ideal path along LOS (meters)

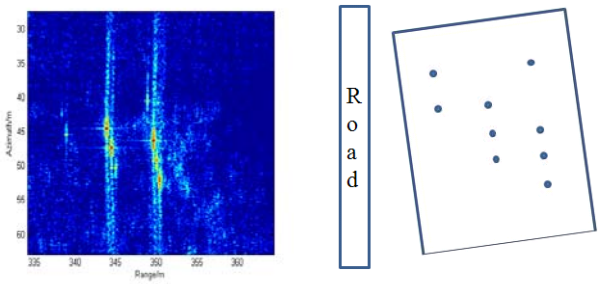

(b) SAR imaging result with motion corrected and schematic diagram of corner reflectors

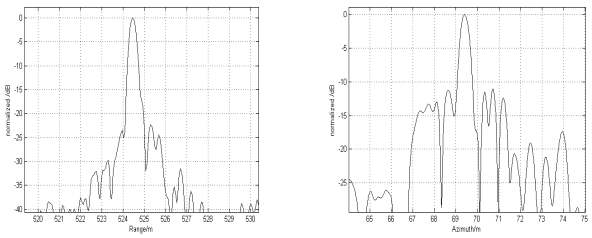

(c) The range and azimuth profile comparison

Figure.7. The processed SAR image with a 600-MHz bandwidth FMCW SAR on a SUV.

in the scene. With the imaging process chart shown in Fig.3, we obtained the results shown in Fig.7. From the above to down: (a) the measured motion error calculated from the GPS data. (b) the focused image after applying the proposed compensation scheme and the schematic diagram of corner reflectors.(c) the range and azimuth profile.

From Fig.7, it is obvious that the corner reflector is well focused. The amplitude is various because the off-nadir angle is approximate to zero so the variance of corner reflectors' placement has a significant influence on the radar cross section (RCS). In addition, the integrated side lobe rate of azimuth compression is higher than the ideal case, since the motion error contains high-frequency component which is hard to compensation based on GPS data. However, some autofocus approaches, such as PGA [9]-[10] and PACE [11] could improve the result of compression.

From the simulated and experimental result shown in Fig. 6, Fig. 7 and Fig. 8, it is obvious that the SAR is well focused, further, the proposed approach is valid. While more high-precise high-resolution large scene airborne based FMCW SAR data focusing is ongoing. It is confident that the high resolution SAR imagery will have a vast application in kinds of fields. Like remote sensing, monitor, cartography, disaster estimation, environment survey.etc.

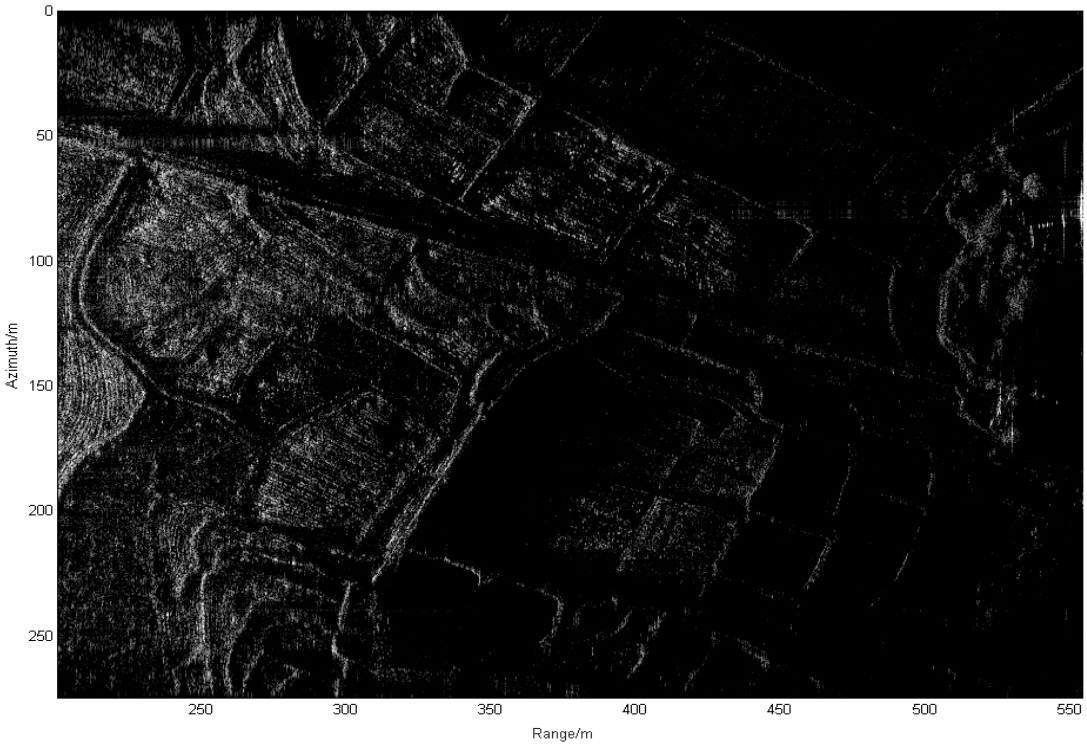

Figure.8. Focused FMCW SAR imagery processed with the proposed method. The scene is a paddy field, it is seen that the ridge and the alley of field are clear. In addition, the texture of reaped rice field is clear too.

V. CONCLUSION AND FUTURE WORK

The main difference between pulsed SAR and FMCW SAR is the approximation stop-go is invalid and the motion during inter-pulse should be considered. Hence the traditional motion compensation method which is suitable for pulsed SAR will no longer available for FMCW SAR. An available method for FMCW SAR motion compensation is proposed in this paper. The geometry and signal model of FMCW SAR in the presence of 3-D motion error is built; the influence introduced by inter-pulse motion error is analyzed while the accordingly approach is presented too. Simulated FMCW SAR data is generated and the proposed method is compared to traditional method. Simulation shows the proposed method results are much better than those of traditional method and the proposed method is particularly available for FMCM SAR. Eventually, the proposed approach is adopted on a laboratorial FMCW SAR system. Well-focused experimental data confirm the effectiveness of the presented method.

REFERENCES

[1] A. META. “Signal Processing of FMCW Synthetic Aperture Radar Data”. Delft University of Technology, Ph.D.thesis, 2005.

[2] A. META, P. Hoogeboom and L.P. Ligthart. “Signal Processing for FMCW SAR”. IEEE Trans on GRS.vol. 45.2007, pp. 3519 -3532.

[3] R. Wang, O. Loffeld, and H. Nies. “Focus FMCW SAR Data Using the Wave number Domain Algorithm ”. IEEE Trans on GRS. Vol. 48. 2010, pp. 2109 – 2118.

[4] J.J.M.deWit, A. Meta, and P.Hoogeboom. “Modified Range-Doppler Processing for FMCW Synthetic Aperture Radar ”. IEEE GRS Letters,vol. 3. 2006, pp.83-87.

[5] A.Ribalta. “Time-Domain Reconstruction Algorithms for FMCW-SAR ”. IEEE GRS Letters.vol. 8. 2011, pp.396-400.

[6] G.FORNARO. “Trajectory Deviations in Airborne SAR: Analysis and Compensation ”.IEEE Trans on AES.vol. 35.1999, pp. 997 - 1009.

[7] A. META, P.Hoogeboom, and L.P. Ligthart. “Non-linear Frequency Scaling Algorithm for FMCW SAR Data”. Proceedings of the 3rd European Radar Conference.2006, pp.9-12.

[8] E. C. Zaugg and D. G. Long. “Theory and Application of Motion Compensation for LFM-CW SAR”. IEEE Trans on GRS. vol. 46. 2008, pp.2990-2998.

[9] H.L.Chan and T.S.Yeo. “Noniterative Quality Phase Gradient Autofocus (QPGA) Algorithm for Spotlight SAR Imagery”. IEEE Trans on GRS. vol. 36. 1998, pp.1531-1539.

[10] W.L.Van Rossum and M .P.G. Otten. “Extended PGA for Range Migration Algorithms”. IEEE Trans on AES, Vol. 42. APRIL2006, pp.478-488.

[11] J.Kolman. “PACE: an autofocus algorithm for SAR”. Virginia, USA, 2005, pp.310-314.

 ISBN: 978-1-61208-264-6